International Journal of Mass Spectrometry 377 (2015) 101–108

Contents lists available at ScienceDirect

International Journal of Mass Spectrometry

journal homepage: www.elsevier.com/locate/ijms

Bond-forming reactions of N_2^{2+} with C_2H_4, C_2H_6, C_3H_4 and C_3H_6

James D. Fletcher, Michael A. Parkes, Stephen D. Price *

Department of Chemistry, University College London, 20 Gordon Street, London, WC1H 0AJ, UK

ARTICLE INFO

Article history:
Received 13 March 2014
Received in revised form 10 May 2014
Accepted 15 May 2014
Available online 23 May 2014

Keywords:
Dication
Ion-molecule reactions
Hydride transfer
Titan
Reaction dynamics

ABSTRACT

Mass spectrometry, coupled with position-sensitive coincidence detection, has been used to investigate the reactions of N_2^{2+} with various small hydrocarbon molecules (C_2H_4, C_2H_6, C_3H_4, c-C_3H_6 and n-C_3H_6) at collision energies below 10 eV in the centre-of-mass frame. The reactivity, in each case, is dominated by electron transfer. However, in each collision system we also clearly identify products formed following the creation of new chemical bonds. These *bond-forming reactions* comprise two distinct classes: (i) hydride transfer reactions which initially form N_nH^+ ($n = 1, 2$) and (ii) N^+ transfer reactions which form monocationic products with C—N bonds. These bond-forming reactions make a small (5–10%), but significant, contribution to the overall product ion yield in each collision system. The temporal and positional data recorded by our coincidence detection technique are used to construct scattering diagrams which reveal the mechanisms of the bond-forming reactions. For the hydride transfer process, the scattering diagrams reveal that H^- is directly transferred from the hydrocarbon to N_2^{2+} at significant interspecies separations. For the hydride transfer reactions with C_2H_4, C_2H_6 and C_3H_4, we observe fragmentation of the nascent N_2H^{+*} to form $NH^+ + N$. The N^+ transfer reaction also proceeds by a direct mechanism: a single step involving N^+/H exchange results in the formation of a singly-charged organic species containing a C—N bond which is detected in coincidence with H^+. The two general classes of bond-forming reactivity we observe in the reactions of N_2^{2+} with organic molecules may be relevant in the chemistry of energised environments rich in molecular nitrogen and hydrocarbon species, such as the atmosphere of Titan.

1. Introduction

Chemical modelling has predicted that N_2^{2+} is present in the nitrogen-rich ionosphere of Titan, the largest of Saturn's moons [1]. Although the electronic states of most small molecular dications are thermodynamically unstable, due to the close proximity of the two like charges, it has long been known that many of these doubly-charged species possess long-lived metastable states with significant barriers to dissociation [2–4]. In fact, the lifetime of the ground electronic state of N_2^{2+} is of the order of at least several seconds [5], and the abundance of N_2^{2+} in Titan's atmosphere is predicted to be comparable to that of some significant singly-charged species, such as CN^+ and C_2H^+ [1]. Thus, in environments such as planetary ionospheres, N_2^{2+} will exist for a sufficiently long time to collide with other molecules and may be involved in a wide range of chemical and physical processes [6]. Importantly, in addition to the possibility of new species being directly formed following N_2^{2+} collisions with other molecules, bimolecular reactions involving dications and neutrals often result in the formation of pairs of singly-charged ions [7,8]. These product monocations are usually highly translationally energetic, due to their mutual Coulomb repulsion, and can subsequently collide with other molecules. In such encounters, the additional translational energy of the products of dication reactions can allow nominally endothermic reactions to proceed. Given these considerations, there exists the possibility of a rich chemistry in energised media where dicationic species are present [3,7,9–14].

In addition to molecular nitrogen, methane (CH_4) and other small hydrocarbons including acetylene (C_2H_2), ethylene (C_2H_4), ethane (C_2H_6) and propane (C_3H_8) are present in the atmosphere of Titan [15]. The reactivity of N_2^{2+} with several of these neutral species has been documented in a recent review article by Dutuit et al. [6]. Summarising this experimental work, Lilensten et al. have studied low energy collisions between N_2^{2+} and CH_4, focusing on the kinetics of electron recombination and the identification of chemical reaction products [1,16]. In the same study, the chemical reactions following collisions between N_2^{2+} and C_2H_4 were also investigated [16]. In both collision systems, electron transfer processes have been identified as the primary reaction channels. However, contributions from bond-forming reactivity were also reported. Specifically, following the low energy N_2^{2+}/CH_4 collisions NH^+, NH_2^+, HCN^+ and H_2CHN^+ were detected [1,6,17]. Similarly,

* Corresponding author. Tel.: +44 2076794606.
E-mail address: s.d.price@ucl.ac.uk (S.D. Price).

http://dx.doi.org/10.1016/j.ijms.2014.05.009

following collisions of N_2^{2+} with $C_2H_4(C_2D_4)$, a range of cations (NH^+, NH_2^+, HCN^+ and H_2CHN^+) resulting from bond-forming chemistry were detected [6]. However, as acknowledged by the authors, these pioneering preliminary investigations pointed to the need for a coincidence experiment to unravel the detailed form of the chemical reactivity. The investigation of the reactivity of N_2^{2+} with $C_2H_4(C_2D_4)$ discussed above is the only investigation, to date, of the chemistry occurring following collisions between N_2^{2+} and the small hydrocarbons which are the targets of this study (C_2H_4, C_2H_6, C_3H_4, n-C_3H_6 and c-C_3H_6).

Considering coincidence studies of the reactivity of N_2^{2+}, Lockyear et al. investigated the chemistry following N_2^{2+}/H_2 collisions using mass spectrometry coupled with position-sensitive coincidence (PSCO) detection [18]. Extensive single (SET) and double (DET) electron transfer reactivity were observed, in addition to bond-forming chemistry leading to the formation of NH^+. Here, the kinematics extracted from the coincidence data revealed that the bond-forming process generating NH^+ proceeds *via* a short-lived collision complex, $[N_2H_2]^{2+}$. Specifically, the reactants associate to form $[N_2H_2]^{2+}$, a neutral N is then lost and the resulting $[NH_2]^{2+}$ dissociates to form NH^+ and H^+. Previous investigations of the reactions of N_2^{2+} with O_2 and C_2H_2 also reveal significant bond forming reactivity [19,20].

The work reported in this article focuses on the dynamics of the bond-forming reactions which occur following collisions between N_2^{2+} and five low mass hydrocarbons: C_2H_4, C_2H_6, C_3H_4 and two isomers of C_3H_6 (propene and cyclopropane). In these collision systems, we clearly identify two types of bond-forming reaction which form pairs of singly charged ions: nitrogen (N) transfer and hydride (H^-) transfer [1,16]. The PSCO detection technique, coupled with time-of-fight mass spectrometry (TOFMS), employed in this investigation detects and unambiguously identifies the pairs of ions formed in individual dicationic reactive events. This coincident detection completely characterises the dicationic reactivity to a depth difficult to achieve using simple mass spectrometric detection [6]. From the timing and positional data that accompany each ion pair detected by the PSCO experiment, we also extract the product ion velocities. The correlations between the product velocities present in this coincidence data, as revealed by scattering diagrams, indicate that both N^+ transfer and H^- transfer reactions proceed by direct mechanisms in all five of the collision systems under investigation. We note that the products of H^- transfer are markedly more intense than those from N^+ transfer in all the collision systems investigated, and a simple mechanistic explanation for this observation is presented.

2. Experimental

The apparatus and methodology involved in our PSCO–TOFMS experiments have been presented in detail in previous publications, therefore only a brief description is provided here [19–25]. In our experiments, N_2 gas, from a commercial source, used without any additional purification, is ionised by 200 eV electrons in a specially-designed source. The resulting ions are extracted from the ion source and focused by a series of electrostatic lenses. This focused beam of singly and multiply charged ions from the source is then energy selected by a hemispherical analyser. The pass energy of the hemisphere is set so that the translational energy spread of the resulting ion beam is approximately 0.3 eV. Upon exiting the hemisphere the beam passes between a set of deflector plates which rapidly sweep the ions across an aperture, forming pulsed, spatially-compact ion 'packets'. The ions are then focused by another set of lenses before entering a commercial velocity filter which, due to the low kinetic energy spread of the ions, selects the ion of interest on the basis of its mass-to-charge ratio (m/z) [26]. In this case, since N^+ and N_2^{2+} both have the same m/z value, the reactant ion beam we employ will be a mixture of these two species. This N^+ contaminant in our dication beam does not prove a problem, however, as reactions of N_2^{2+} can easily be distinguished from those of N^+ using our coincidence technique, as is discussed below.

After passing through the velocity filter, the mass-selected ion beam is decelerated to the chosen collision energy, typically around 8 eV in the laboratory frame. Low collision energies are used in order to increase the probability of forming new chemical bonds during ion-molecule collisions by maximising the ion-molecule interaction time. The pulsed ion beam then encounters an effusive jet of neutral reactant gas in the source region of a linear TOF–MS with second-order space-focusing capability [27]. The hydrocarbon collision gases used in this study were commercial samples (>99% purity) and were used without any additional purification.

Single-collision conditions are maintained in the TOF–MS source region, which is initially field-free, by operating at low neutral gas pressures ($<10^{-6}$ Torr). As the dication packet reaches the centre of the TOF–MS source region, a positive potential is applied to a repeller plate to propel all the product ions and any unreacted dications into the acceleration region of the TOF–MS, and then on into the drift tube. At the end of the drift tube the ions strike a position-sensitive detector (PSD) which is configured to receive multiple ion hits during each mass spectrometric timing cycle. Timing commences shortly after the repeller plate pushes the ions into the acceleration region of the TOF–MS. The PSD is a commercial device, composed of a pair of multi-channel plates and a wire-wound delay-line anode [28]. The front of the detector is held at a large negative potential in order to accelerate all incoming ions to a large impact velocity and hence avoid any mass discrimination effects.

Detector signals resulting from the impact of an ion are discriminated against electrical noise and sent to a time-to-digital converter. For events where two ions are detected (an ion pair), both the arrival time and the position of arrival in the plane of the detector are recorded for each product. These pair events can be classified as either 'real' or 'false' coincidences. 'Real' coincidences involve the detection of two singly-charged ions from the same reactive event, whereas 'false' coincidences involve the detection of two 'unrelated' product ions. Only ion-molecule reactions involving the N_2^{2+} reactant will contribute to the 'real' coincidence data. That is, the vast majority of reactions involving N_2^{2+} will produce a pair of monocations, whilst reactions of the N^+ 'impurity' in the ion beam will only form a single monocationic product. Events resulting in the detection of a single ion will not be added to the coincidence dataset and thus the N^+ ions in our reactant beam do not obscure the dicationic reactivity. However, the significant number of N^+ ions in the beam does increase the number of 'false' coincidences. That is, there is a small probability of detecting an N^+ ion from the beam together with a product ion from a dication reaction. These 'false' pairs involving reactant N^+ ions have a narrow range of flight times that can be easily distinguished from 'real' pairs from dication reactions, as, due to the large Coulomb repulsion between the products, the real pairs are formed with a much broader range of flight times. Thus, to suppress the collection of false coincidences, ion pairs in which one ion in the pair has a flight time very close (±150 ns) to $m/z = 14$ are excluded from the pairs data. Due to their narrow range of flight times, these false pairs can be removed from the coincidence data without losing a significant number of real pairs. A single experiment typically involves recording the arrival times for more than 10^5 pair events. Thus, data acquisition takes several days since, in order to minimise the occurrence of false coincidences, we operate at ion beam intensities which result in the detection of considerably less than one ion for every pulse of the repeller plate. False coincidences involving ions whose masses fall outside the exclusion region have a much lower probability of occurring. However, such false coincidences can

easily be distinguished from real signals as they exhibit a characteristic circular peak shape in the pairs spectrum due to the absence of any correlation between the velocities of the detected ion pair [25].

The time and positional data characterising the detected ion pairs are simply stored during the experiment and then processed and analysed off line. Initially, a two-dimensional histogram of the flight times of the ions detected as pairs (a *pairs* spectrum) is constructed to visualise the coincidence data. These pairs spectra readily identify all the reactions from a given collision system that generate a pair of product monocations. Pairs of singly-charged products resulting from reactive events caused by N_2^{2+} collisions appear as distinct peaks in the pairs spectrum. Each of these peaks can be selected in turn, and the TOF and positional data for the ion pairs making up an individual peak are extracted from the main dataset and can be subjected to further kinematic analysis. As described before in the literature, the flight times and positional data for the two ions ($i = 1, 2$) are used to derive each ion's nascent laboratory-frame (LAB) velocity v_i, for each reactive event we detect [7,25]. These values of v_i can then be converted into centre-of-mass (CM) frame velocities w_i using the velocity of the centre-of-mass of the system v_{cm}: $w_i = v_i - v_{cm}$. The value of v_{cm} can be derived either from the known velocity of the reactant dication or from the LAB frame velocities of the products of a two body reaction (*e.g.* $N_2^{2+} + X \rightarrow N_2^+ + X^+$) [25]. These two methods of deriving the velocity of the CM produce values in good mutual agreement. Using the above methodology our coincidence dataset yields the CM velocities of the pair of monocations formed in every individual reactive event we detect. We then examine these velocities to study the dynamics of the individual reactions.

Many dicationic reactions produce a neutral body in addition to a pair of monocations; they are *three-body* processes. In the CM frame, the CM of the collision system is stationary and the sum of the linear momenta of the products in that frame is equal to zero. Thus, for three-body events, given the experimentally derived velocities for the two monocations (w_1 and w_2), we can derive the CM velocity vector of the neutral third body w_3, completely characterising the kinematics of these reactions. It is important to note however that the neutral's CM velocity can only be derived if just one neutral species is formed, together with the two monocationic species. That is, in principle, the complete kinematics of four-body (or higher order) processes are not accessible to the PSCO technique, although, as shown below, a significant amount of information concerning the reaction dynamics is still available from the PSCO data for these more complex reactions.

For a given reactive process revealed in the pairs spectrum, the values of, and correlations between, the values of w_i can be investigated to probe the dynamics of that reaction. For such an investigation, a series of scattering diagrams, constructed from the product velocity vectors, have proven a powerful way to reveal and visualise the motions of the reaction products [25]. The generation of such scattering diagrams and their interpretation are discussed in greater detail below.

3. Results and discussion

We observe extensive single and double electron transfer reactivity (SET and DET) in all five of the dication/molecule collision systems we have investigated (Table 1). As highlighted above, we have also identified two general types of bond-forming reaction, that accompany these electron transfer reactions: (i) H^- transfer from the hydrocarbon to the dication forming a new N—H bond and (ii) transfer of N^+, resulting in the formation of two singly-charged species, one of which has a C—N bond. The hydride transfer reactions can be further divided into processes which form NH^+ and those which form N_2H^+. Table 1 summarises the product ions formed following these classes of bond-forming reaction for each collision system. Since the SET and DET reactions of dications have been studied extensively, and are both now relatively well understood, our analysis and discussion is focused on understanding the two classes of bond-forming reaction that we observe [22,23,29,30]. Table 1 shows that N^+ transfer makes a relatively small contribution to the dicationic reactivity, with a branching ratio ranging between 0.1% for N_2^{2+} collisions with propene and cyclopropane, to 0.9% for collisions with ethene. In contrast, to the low yield from N^+ transfer reactions, hydride transfer contributes between 5% and 7% of the product ion yield in these collision systems. We note that the dominant contribution of electron transfer to the ion yield from N_2^{2+}/C_2H_4 collisions has been noted before in the pioneering experiments of Thissen et al. [6,17]. Satisfyingly, these authors also noted the formation of NH^+ in this collision system, in accord with our data (Table 1), although our pairs spectra do not reveal any H_nCN^+ products.

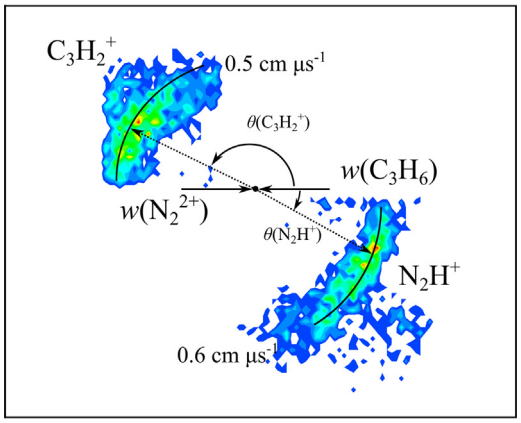

Fig. 1. The CM scattering diagram for the reaction $N_2^{2+} + n\text{-}C_3H_6 \rightarrow C_3H_2^+ + N_2H^+ (+3H)$, recorded at $E_{cm} = 7.2$ eV. As described in the text, the scattering angles for $C_3H_2^+$ and N_2H^+ are shown relative to the direction of v_{cm} which is closely aligned with the CM velocity of the incident dication, $w(N_2^{2+})$. The black dot indicates the position of the CM.

As mentioned above, in order to identify the mechanisms of the bond-forming reactions we look for correlations between the product and reactant velocities in different frames of reference: the CM frame and the 'internal' frame [20,25]. The product velocity vectors, derived from the coincidence data, as described above, are used to construct scattering diagrams in these two frames of reference. For a given reactive channel, we initially construct a 'CM scattering diagram' from the set of reactive events selected. This CM scattering diagram is a radial histogram where, for each w_i, the radial co-ordinate is $|w_i|$ and the angular co-ordinate is the scattering angle ($0^\circ \leq \theta \leq 180^\circ$) between w_i and the direction of v_{cm}. The data for one product ion can be plotted in the upper semi-circle of such a CM scattering diagram and the data for another product in the lower semi-circle. For example, in Fig. 1 the data for $C_3H_2^+$ is plotted in the upper half of the diagram, the data for N_2H^+ is plotted in the lower half. Since, in the LAB frame, the dication velocity is significantly greater than the velocity of the neutral target species, the direction of v_{cm} is very close to that of the incident dication beam.

The second form of scattering diagram is constructed in the 'internal frame'. This second class of diagram is again a radial histogram, but here the scattering of one product's velocity vector is displayed relative to the direction of the velocity of another reaction product. That is, for a given product velocity (w_i) we plot $|w_i|$ as the radial co-ordinate but the angular coordinate is the angle between w_i and the CM velocity of another product ion which has been chosen as the reference for the diagram. In an internal frame scattering diagram, correlations between the individual product ion

Table 1
The bond-forming reactions observed following collisions between N_2^{2+} and five small hydrocarbons. The branching ratio *R* is shown in parentheses for each reaction channel.[a]

Reactants	E_{cm}/eV	N^+ addition product ions (*R* %)	Hydride transfer product ions (*R* %)
$N_2^{2+} + C_2H_4$	6.0	$C_2N^+ + H^+$, $C_2HN^+ + H^+$, $C_2H_2N^+ + H^+$ (0.9)	$C_2H_3^+ + NH^+$ (5)
$N_2^{2+} + C_2H_6$	8.3	$C_2N^+ + H^+$, $C_2HN^+ + H^+$, $C_2H_2N^+ + H^+$ (0.4)	$C_2H_3^+ + NH^+$ (6)
$N_2^{2+} + C_3H_4$	9.4	$C_3H_2N^+ + H^+$ (0.6)	$C_3H_2^+ + NH^+$, $C_3H_3^+ + NH^+$ (7)
$N_2^{2+} + n\text{-}C_3H_6$	7.2	$C_3HN^+ + H^+$, $C_3H_2N^+ + H^+$ (0.1)	$C_3H_3^+ + NH^+$ (2)$C_3H^+ + N_2H^+$, $C_3H_2^+ + N_2H^+$ (3)
$N_2^{2+} + c\text{-}C_3H_6$	7.2	$C_3H_2N^+ + H^+$ (0.1)	$C_3H_3^+ + NH^+$ (2)$C_3H^+ + N_2H^+$, $C_3H_2^+ + N_2H^+$ (3)

[a] For reactions which differ only in the number of hydrogen atoms bound in the products, a composite branching ratio including all such products is presented.

velocities themselves can be examined. Again, since the scattering angles range between 0° and 180°, the data for two different product ions can be plotted in the upper and lower halves of the diagram. In the analysis presented below, these two classes of scattering diagram are used to explore the reaction mechanisms of the bond-forming channels listed in Table 1.

3.1. Hydride transfer

In all of the collision systems investigated, we observe hydride transfer from the hydrocarbon species to the dication to form either N_2H^+ or NH^+ in coincidence with a carbocation. Of course, these products, N_2H^+ and NH^+, have the same nominal *m/z* values as $^{15}N^{14}N^+$ and $^{15}N^+$, respectively (29 and 15). However, given the significant (Table 1) abundance of these product ions, and the fact that the relative abundance of $^{15}N^{14}N^{2+}$ in our ion beam (recall that the ion beam is mass selected at *m/z* = 14) will be much less than the natural relative abundance of ^{15}N (~0.4%) [31], we can unambiguously conclude these product ion signals are due to hydride transfer to $^{14}N_2^{2+}$ to form N_2H^+ and NH^+. We discuss the formation of the two products of hydride transfer (N_2H^+ and NH^+) separately below, considering in detail for each ion the dynamics of a representative reactive channel.

3.1.1. $N_2^{2+} + C_3H_6 \rightarrow N_2H^+ + C_3H_2^+$ (+3H)

Scattering diagrams have been constructed, as explained above, in order to explore the kinematics of the H transfer reactions. First we consider the formation of N_2H^+ following collisions between N_2^{2+} and C_3H_6. Of all the organic molecules investigated in this study, only the two isomers of C_3H_6 undergo hydride transfer with N_2^{2+} to form N_2H^+ in coincidence with a carbocation; hydride transfer in the other collision systems forms only NH^+. The strongest channel forming N_2H^+ is observed following N_2^{2+}/propene collisions, where $C_3H_2^+$ is the partner monocation. The $C_3H_2^+$ and N_2H^+ CM velocity vectors following N_2^{2+}/propene collisions are shown in Fig. 1, which reveals the unambiguous signature of strong forward-scattering dynamics. Indeed, strong forward scattering has previously been observed for hydride transfer in other dication collision systems [32]. The forward scattering is characterised by the fact that the direction of $w(N_2H^+)$ is strongly orientated in the same direction as the velocity of the N_2^{2+} reactant from which it is derived. Similarly the direction of $w(C_3H_2^+)$ is strongly orientated with the CM velocity of the C_3H_6 neutral. These forward-scattering dynamics reveal a process where the incoming species interact at relatively large separations and do not combine to form a collision complex [33]. That is, the dication strips a hydride ion from the neutral at relatively large inter-species separations and the product trajectories are then very similar to those of the reactants from which they are derived [33]. If the reaction mechanism were "indirect" the reactants would interact more intimately, and perhaps associate on a longer time scale. In this situation we would expect that the product velocity vectors will be scattered over a wide range of CM scattering angles; that is the product velocities would possess no correlation with the velocities of the reactants. This characteristic "isotropic" scattering, often attributed to the formation of a transitory collision complex, has been observed previously for a number of different dication collision systems [14].

In the formation of N_2H^+ from N_2^{2+}–propene collisions, there may be up to three neutral species accompanying the two product ions. In this situation, as highlighted above, the velocity of the neutral species cannot be determined from the velocities of the product ions. However, the scattering of the product ions in the internal frame, relative to each other, reveals that their velocities are strongly anti-correlated, exactly as would be expected for direct H^- transfer at significant interspecies separations. In summary, the scattering of the product ions, in both the CM and internal frame, provide conclusive evidence that the mechanism for the formation of N_2H^+ and $C_3H_2^+$ is a direct, stripping-style process.

3.1.2. $N_2^{2+} + C_2H_4 \rightarrow NH^+ + C_2H_3^+ + N$

As mentioned above, the N_2H^+ ion is detected only from the reactions of N_2^{2+} with the two isomers of C_3H_6. However, in all of the N_2^{2+} collision systems investigated we detect the formation of NH^+ (Table 1). The N_2^{2+}/C_2H_4 system exhibits the most intense signal for this class of hydride transfer process, forming $C_2H_3^+ + NH^+$, and therefore our detailed analysis focuses on this reaction. The other collision systems forming NH^+ exhibit very similar scattering to that discussed here, and are considered briefly in a later section.

The CM scattering diagram for this reaction (Fig. 2) shows a strong anti-correlation between the $C_2H_3^+$ and NH^+ velocity vectors in the CM frame: NH^+ is forward-scattered in the direction of N_2^{2+} and $C_2H_3^+$ is scattered in the opposite direction, aligned with the motion of C_2H_4. This scattering data clearly shows that the dynamics of the hydride transfer reaction forming NH^+ is analogous to the formation of N_2H^+ discussed above, specifically the process is a direct, stripping-style reaction.

For this reaction, which is a three-body process, we are also able to determine the velocity of the neutral N atom which is formed together with the two singly charged product ions. The internal

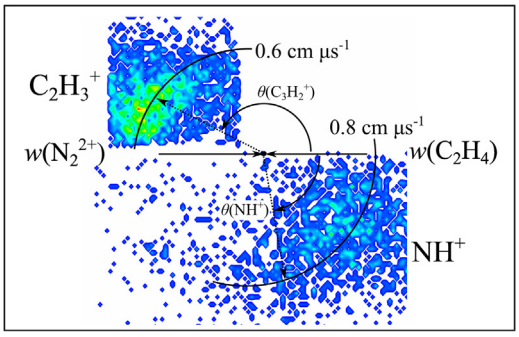

Fig. 2. The CM scattering diagram for the reaction $N_2^{2+} + C_2H_4 \rightarrow C_2H_3^+ + NH^+$ (+N), recorded at E_{cm} = 6.0 eV. The scattering angles for $C_2H_3^+$ and NH^+ are shown relative to the velocity of the incident dication, $w(N_2^{2+})$. See text for details.

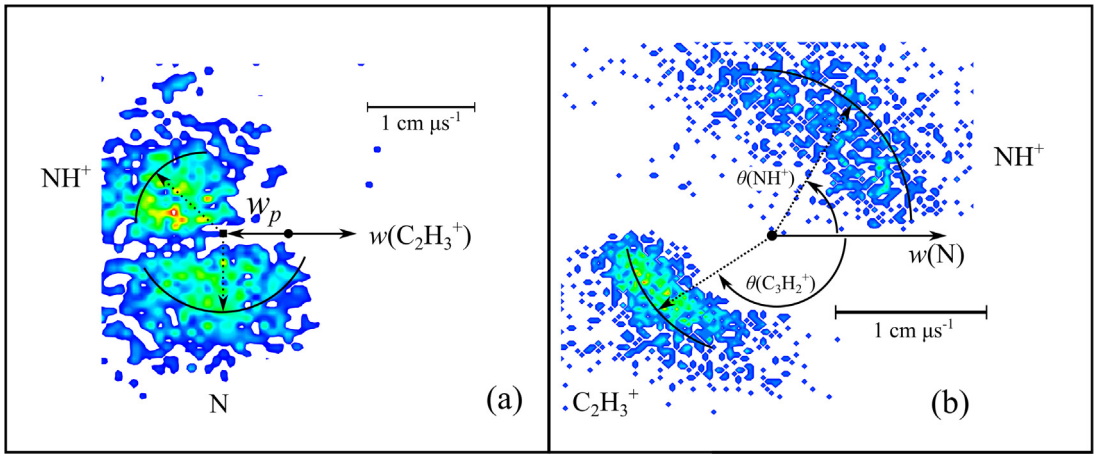

Fig. 3. The internal frame scattering diagram for the reaction $N_2^{2+} + C_2H_4 \rightarrow C_2H_3^+ + NH^+ + N$, recorded at E_{cm} = 6.0 eV. (a) the scattering of N and NH^+ relative to $w(C_2H_3^+)$, the precursor (N_2H^{+*}) velocity w_p is marked; (b) the scattering of NH^+ and $C_2H_3^+$ relative to w(N).

frame scattering diagrams, showing the NH^+, $C_2H_3^+$ and N velocity vectors relative to each other, are presented in Fig. 3.

Fig. 3 shows that the velocities of both NH^+ and N are strongly anti-correlated to the motion of $C_2H_3^+$, further evidence that the reaction proceeds *via* a direct mechanism. In Fig. 3a we see that the NH^+ and N trajectories are scattered about a point markedly backscattered relative to the centre-of-mass. This style of internal frame scattering, which has been observed before, results from a reaction mechanism involving the formation of NH^+ and N *via* dissociation of an energised primary precursor ion (N_2H^{+*}) [18]. This precursor ion is formed in the initial dication-molecule interaction along with the $C_2H_3^+$ ion. The centre of the scattering of the NH^+ ion and the N neutral (marked with a square in Fig. 3a) then corresponds to the velocity of the N_2H^{+*} precursor (w_p, Fig. 3a).

To support these deductions, we note that the modal CM velocity of $C_2H_3^+$ that we determine experimentally is approximately 0.6 cm μs^{-1}. Therefore, if the initial step of the reaction involves the formation of N_2H^{+*} and $C_2H_3^+$, the velocity of the N_2H^{+*} precursor can be calculated, using conservation of momentum, to be just less than 0.6 cm μs^{-1}. This calculated value is in very good agreement with the value of w_p obtained by inspection of the scattering diagram. Given the above analysis, the reaction mechanism for this channel is clearly as shown below (reaction (1)):

$$N_2^{2+} + C_2H_4 \rightarrow N_2H^{+*} + C_2H_3^+ \rightarrow NH^+ + N + C_2H_3^+ \quad (1)$$

The NH^+ and N velocity vectors, originating from the fragmentation of N_2H^{+*}, are both distributed about the same precursor velocity vector (w_p, Fig. 3a), as discussed above, although they exhibit subtly different distributions about that vector. Inspecting Fig. 3a closely, we see that the N fragment is clearly symmetrically scattered about $w(N_2H)^{+*}$, whereas the NH^+ ion appears to be slightly asymmetrically distributed about $w(N_2H)^{+*}$. That is, the NH^+ ion is slightly more strongly scattered (approximately 0.3 cm μs^{-1}) away from the direction of $w(C_2H_3^+)$ than the neutral N atom. Such scattering has been observed before for this sort of sequential reaction mechanism, and is interpreted as the result of a residual Coulombic interaction between the two singly charged products following the dissociation of the N_2H^{+*} precursor [22]. The fragmentation of N_2H^{+*} must take place on a short enough time-scale that the NH^+ ion experiences some Coulomb repulsion from the departing $C_2H_3^+$ product. Given that the NH^+ ion appears to be going about 0.3 cm μs^{-1} faster away from the $C_2H_3^+$ than the neutral N atom (on average) we estimate that the N_2H^{+*} breaks up (on average) when it is approximately 10 Å from the carbocation.

3.2. N^+ transfer

As highlighted above (Table 1), all five collision systems display clear evidence of the transfer of N^+ from the N_2^{2+} dication to the reactant hydrocarbon molecule following N_2^{2+}/neutral collisions. These reactions form new C—N bonds. The branching ratios for these N^+ transfer reactions are all less than 1%. We feel confident in asserting that these low experimental branching ratios reflect the small reaction cross sections of these N^+ transfer channels, rather than arising from major experimental discrimination issues associated with the detection of H^+ ions. Specifically, as highlighted in previous publications, we have established TOFMS settings which minimise both mass and energy discrimination, resulting in a uniform detection efficiency of both products formed as an ion pair, regardless of their identity [34]. Furthermore, if energetic H^+ ions were lost 'sideways' in the mass spectrometer we would see clear gaps in the scattering data reflecting these 'missing' ion trajectories. Such losses are not observed in our scattering diagrams. Further evidence against serious discrimination is that, for the $CF_2^{2+} + H_2O$ collision system, similar branching ratios for the different reactive channels (some involving the formation of H^+) have been measured on the PSCO experiment and another piece of apparatus [35].

We must also be sure these weak signals involving N^+ transfer are due to reactions of low cross section between N_2^{2+} and the relevant neutral molecule, not to reactions of significant cross section with the hydrocarbon impurities (<1%) present in the neutral sample. Any significant contribution to the "N^+ transfer" reaction intensities from reactions of N_2^{2+} with the hydrocarbon impurities can be discounted for two reasons. Firstly, if chemical reactivity with the impurities accounts for the "N^+ transfer" signals, then SET reactions with the impurities should certainly be observed, because in these collision systems SET reactions always have larger cross sections than the chemical channels. No such SET reactivity with the impurity species is visible in any of our coincidence spectra. Secondly, if reactions with the impurity hydrocarbons were important, we would expect to see some reaction channels (chemical or SET) which must unequivocally involve hydrocarbon molecules heavier than the nominal neutral reactant. Again, no such reactivity is detected. The above analysis confirms that the N^+ transfer reactivity we observe is due to the reactions of N_2^{2+} with the major (>99%) component of the neutral collision gas.

Having satisfied ourselves that the experimental branching ratios for the N^+ transfer reactions are a true reflection of the relative reactions cross sections, and that the reactions result from the collisions of N_2^{2+} with the title molecules, we can construct CM

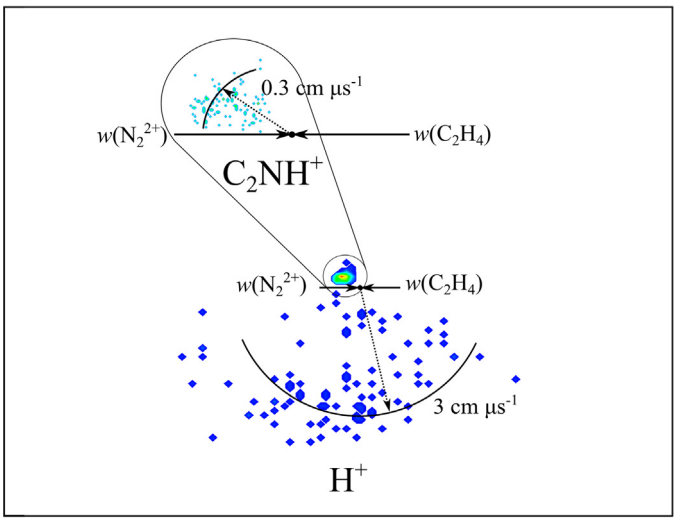

Fig. 4. The CM scattering diagram for the reaction $N_2^{2+} + C_2H_4 \rightarrow C_2NH^+ + H^+(+N+2H)$, recorded at $E_{cm} = 6.0$ eV. The scattering vectors for C_2NH^+ and H^+ are shown relative to the incident dication velocity, $w(N_2^{2+})$. The inset shows the C_2NH^+ scattering on a larger scale.

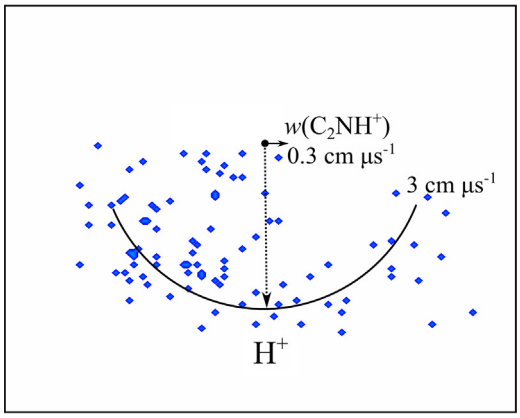

Fig. 5. The internal frame scattering diagram for the reaction $N_2^{2+} + C_2H_4 \rightarrow C_2NH^+ + H^+$ (+N + 2H), recorded at $E_{cm} = 6.0$ eV showing the scattering of H^+ relative to the velocity of C_2NH^+.

scattering diagrams from our data to study the kinematics of these unusual processes.

3.2.1. $N_2^{2+} + C_2H_4 \rightarrow C_2NH^+ + H^+$ (+N + 2H)

Again, we focus our analysis on the N_2^{2+}/C_2H_4 collision system since it exhibits the most intense N^+ transfer reaction. Fig. 4 shows the CM scattering diagram for the reaction which forms $C_2NH^+ + H^+$ following N_2^{2+}/C_2H_4 collisions at $E_{cm} = 6.0$ eV. Peaks corresponding to the $C_2N^+ + H^+$ and $C_2NH_2^+ + H^+$ ion pairs are also visible in the pairs spectrum, but are significantly less intense than the reaction forming C_2NH^+.

In the CM scattering diagram presented in Fig. 4, there is clear evidence that the C_2NH^+ velocity vectors, although tightly grouped near to the CM, are scattered in the same direction as the CM velocity of the C_2H_4 reactant. In contrast, the fast H^+ ions are widely distributed over a large volume of scattering space and, consequently, these data are hard to interpret in detail. Clearly though, the orientation of the C_2NH^+ velocity vectors hints at a direct reaction mechanism.

There are various different combinations of neutral species that could be formed together with $C_2NH^+ + H^+$ (N + 2H, NH + H, N + H_2 or NH_2), which means we cannot derive the motion of the neutral species from the scattering data. Indeed, unfortunately, there are no examples of three-body N^+ transfer reactions in any of the collision systems we have investigated. However, a similar three body reaction has been previously observed following collisions between $N_2^{2+} + C_2H_2$, where two singly-charged ions resulting from an N^+ transfer reaction, H^+ and C_2HN^+, were detected [36]. In this case the reaction must be a three-body process, as the neutral species can only be an N atom, and the CM velocities of all three products could be determined. The product scattering in the N_2^{2+}/C_2H_2 collision system revealed that the mechanism of N addition takes place in two steps. In the first step, a direct N^+/H atom exchange, results in formation of C_2HN^+ and NH^+, which is followed by the subsequent fragmentation of NH^+ to form N + H^+.

The experimental evidence pointing to a direct mechanism for the formation of C_2NH^+ in N_2^{2+}/C_2H_4 collision system (Fig. 4) restricts the possible mechanisms for the N transfer process to two general pathways (reactions (2) and (3)). These possible pathways involve N^{2+} or N^+ transfer to the hydrocarbon respectively. Reactive pathways involving the association of the reactants to form 'long-lived' singly-charged or doubly-charged species (*e.g.* $C_2H_4N_2^{+/2+}$) can be ruled out by the experimental data pointing strongly towards a direct mechanism.[7] That is, the expected decoupling of $w(C_2NH^+)$ from $w(C_2H_4)$ characteristic of a reaction mechanism involving 'complexation' is clearly not present in Fig. 4.

$$N_2^{2+} + C_2H_4 \rightarrow C_2H_4N^{2+*} + N \rightarrow C_2HN^+ + H^+ + N + [2H] \quad (2)$$

$$N_2^{2+} + C_2H_4 \rightarrow C_2H_3N^+ + NH^{+*} \rightarrow C_2HN^+ + N + H^+ + [2H] \quad (3)$$

To determine which of the above pathways best describes the mechanism of the N^+ transfer reaction we can look at the scattering of $w(H^+)$ relative to $w(C_2HN^+)$, as shown in Fig. 5. In Fig. 5, we clearly see that the H^+ scattering does not exhibit any strong correlation with $w(C_2NH^+)$, indicating that the motion of H^+ is not coupled to the motion of C_2HN^+. This scattering pattern is evidence that H^+ and C_2HN^+ are not derived from a $C_2H_4N^{2+*}$ precursor, as in reaction (2). In fact, if reaction (2) was taking place, we would expect the H^+ and C_2HN^+ velocity vectors to be highly anti-correlated in the internal frame, as the charged products of the fragmentation of $C_2H_4N^{2+*}$ would separate with strongly anti-correlated momenta [19].

Having eliminated reaction (2) as a possible mechanism for 'N^+ transfer' this leaves us with reaction (3). Satisfyingly, reaction (3) is perfectly analogous to the N^+ transfer mechanism unambiguously identified in the N_2^{2+}/C_2H_2 collision system in earlier work [36]. In reaction (3), $C_2H_3N^+$ and NH^{+*} form in an initial, direct, N^+/H exchange step. As the two products of this exchange ($C_2H_3N^+$ and NH^{+*}) separate, they will rotate independently, decoupling the velocities of the products of the fragmentation of NH^{+*} (N and H^+) from the velocities of the products of the fragmentation of $C_2H_3N^+$ ($C_2HN^+ + 2H$). Reaction (3) should therefore give rise to no correlation between the velocities of H^+ and C_2HN^+, just as we observe in Fig. 5. Therefore, given the scattering in both the CM and internal frames of reference, and the previous work on the N_2^{2+}/C_2H_2 collision system, we are satisfied that reaction (3) provides a good description of the N^+ transfer reaction in the N_2^{2+}/C_2H_4 collision system.

The branching ratios for H^- transfer are significantly greater than those for N^+ transfer in all of the collision systems investigated (Table 1). Since we have identified direct reaction mechanisms for both processes, it appears that dynamic effects, rather than the thermodynamic stabilities of the products, should have the greater influence on these relative ion yields. Indeed it seems reasonable that the transfer of H^-, a single light species, in a direct reaction should be much more facile than the complex inter-exchange of N^+/H in the N^+ transfer process.

3.3. Other N_2^{2+} collision systems

Where we have sufficiently intense PSCO data, we have also analysed the scattering patterns for N^+ transfer and hydride transfer in the collision systems listed in Table 1 that have not been discussed in detail above. The scattering diagrams in each case are very similar to the representative examples presented in earlier sections. These individual collision systems are discussed briefly below.

3.3.1. $N_2^{2+} + C_2H_6$

Products from N^+ transfer reactions channel are clearly evident in the pairs spectrum following N_2^{2+}/C_2H_6 collisions at E_{cm} = 8.3 eV. The most intense reaction of this type corresponds to the formation of $C_2NH_2^+$ in coincidence with H^+. The product velocities, viewed in the CM frame, again indicate that this reaction proceeds *via* a direct mechanism as described above for N_2^{2+}/C_2H_4. N^+ transfer products with fewer hydrogen atoms on the carbon backbone are also weakly visible ($C_2N^+ + H^+$, $C_2NH^+ + H^+$), but the scattering is less clear for these weaker channels. The branching ratio for N^+ transfer in this collision system is 0.4%, less than half the yield of the analogous reaction involving C_2H_4. This difference in yield perhaps arises because the greater localised electron density of the double bond in C_2H_4 facilitates the addition of N^+ to the unsaturated hydrocarbon.

In the N_2^{2+}/C_2H_6 collision system, we also observe hydride transfer yielding NH^+ in coincidence with $C_2H_3^+$. Again, we cannot extract the CM velocities of the neutral(s) for this reaction as it is potentially a four-body process. Considering the CM scattering of NH^+ and $C_2H_3^+$, the product ion velocities are strongly aligned with the reactants from which they are derived. Thus, this hydride transfer clearly proceeds *via* the direct mechanism identified above.

3.3.2. $N_2^{2+} + C_3H_4$

An N^+ transfer reaction channel is observed in the pairs spectrum following N_2^{2+}/C_3H_4 collisions at E_{cm} = 9.4 eV. The products formed in coincidence are C_3NH^+ and H^+ and a significantly weaker peak corresponding to $C_3N^+ + H^+$. The branching ratio for this reaction (0.6%) is slightly less than for the N^+ transfer reaction following N_2^{2+}/C_2H_4 collisions, but greater than the N_2^{2+}/C_2H_6 system (Table 1). Again, the significant electron density in the triple bond may play a role in facilitating the N^+ transfer reaction in this system.

The scattering of C_3NH^+ and H^+ in the CM frame is again indicative, as described above, of a direct N^+ transfer reaction: $w(C_3NH^+)$ is broadly aligned with the N_2^{2+} velocity and H^+ is scattered over a large range of scattering angles. As discussed above, this scattering is in accord with a direct N^+/H exchange step followed by the fragmentation of the primary NH^{+*} product.

The hydride transfer reaction that we observe following N_2^{2+}/C_3H_4 collisions results in the formation of a single neutral body (N) in addition to two monocations ($C_3H_3^+ + NH^+$). The internal frame scattering diagram in Fig. 6 shows $w(NH^+)$ and $w(N)$ plotted relative to $w(C_3H_3^+)$. In Fig. 6 we observe the general scattering motif that was described above for H^- transfer following N_2^{2+}/C_2H_4 collisions. Specifically, H^- transfer produces N_2H^{+*}, and this ion then dissociates to form $NH^+ + N$. In the internal frame scattering diagram (Fig. 6), the $NH^+ + N$ fragments are scattered about a point corresponding to $w(N_2H^{+*})$. In this collision system, however, $w(NH^+)$ and $w(N)$ are both symmetrically distributed about $w(N_2H^{+*})$. This symmetrical scattering implies that the fragmentation of N_2H^{+*} occurs outside the Coulomb field of the carbocation. Hence, we conclude that the fragmentation of $N_2H^{+*}$is less rapid following N_2^{2+}/C_3H_4 collisions than N_2^{2+}/C_2H_4 collisions.

3.3.3. $N_2^{2+} + C_3H_6$

The N_2^{2+}/propene and N_2^{2+}/cyclopropane collision systems both exhibit weak N^+ transfer channels. The scattering diagrams for these weak reactions are harder to interpret, but there are again hints that the direct N^+ transfer mechanism identified above is taking place. The branching ratios of N^+ transfer following N_2^{2+}/C_3H_6 collisions are the weakest observed in this investigation (<0.1%). This distinct reduction in N^+ transfer reactivity observed for propene, despite the presence of a double bond, may be caused by an increased probability of electron transfer in these collision systems which involve a larger neutral molecule with a lower ionisation energy. Indeed, the branching ratios for electron transfer in both of the $N_2^{2+} + C_3H_6$ collision systems exceed those for all the other collision systems investigated here.

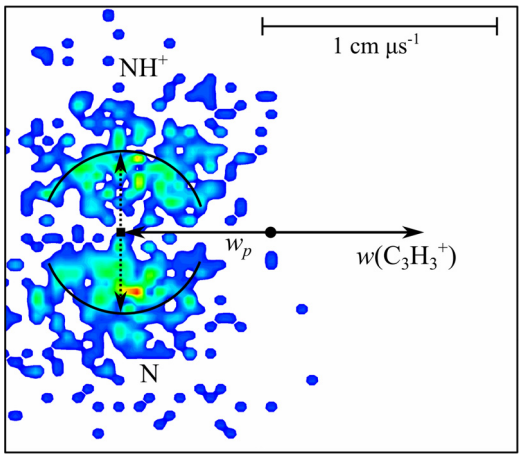

Fig. 6. The internal frame scattering diagram for the reaction $N_2^{2+} + C_3H_4 \rightarrow C_3H_3^+ + NH^+$ (+N), recorded at E_{cm} = 9.4 eV. The scattering of N and NH^+ is shown relative to the velocity of $C_2H_3^+$. The velocity w_p of the N_2H^{+*} precursor, which fragments to $NH^+ + N$, is also shown.

As described above, the scattering of N_2H^+ and $C_3H_2^+$ following N_2^{2+}/propene collisions indicates that H^- is transferred in a rapid, direct reaction. Similar scattering is also observed for the same products following N_2^{2+}/cyclopropane collisions. For the formation of NH^+, generated by H^- transfer, following N_2^{2+}/C_3H_6 collisions, we again see clear evidence (for both isomers) of direct H^- transfer followed by fragmentation of N_2H^{+*}, as described for the N_2^{2+}/C_2H_4 collision system.

4. Conclusions

The reactions of N_2^{2+} with C_2H_4, C_2H_6, C_3H_4 and two isomers of C_3H_6 have been investigated at collision energies of less than 10 eV in the centre-of-mass frame. Electron transfer reactions dominate the product ion yield. However, pathways to forming NH^+ and N_2H^+ (hydride transfer) and C—N bonds (N^+ transfer) have been clearly identified. Both reactions proceed *via* direct mechanisms.

Acknowledgements

The support of the EPSRC for these experiments is gratefully acknowledged. JDF acknowledges the financial support of the UCL "Impact Scheme".

References

[1] J. Lilensten, O. Witasse, C. Simon, H. Soldi-Lose, O. Dutuit, R. Thissen, C. Alcaraz Geophys, Res. Lett. 32 (2005) L03203.
[2] A.L. Vaughan, Phys. Rev. 38 (1931) 1687.
[3] S.D. Price, J. Chem. Soc. Faraday Trans. 93 (1997) 2451.
[4] D. Mathur, Phys. Rep. 391 (2004) 1.
[5] D. Mathur, L.H. Andersen, P. Hvelplund, D. Kella, C.P. Safvan, J. Phys. B 28 (1995) 3415.
[6] O. Dutuit, N. Carrasco, R. Thissen, V. Vuitton, C. Alcaraz, P. Pernot, N. Balucani, P. Casavecchia, A. Canosa, S.L. Picard, J.-C. Loison, Z. Herman, J. Zabka, D. Ascenzi, P. Tosi, P. Franceschi, S.D. Price, P. Lavvas, Astrophys. J. Suppl. S 204 (2013) 20.

[7] S.D. Price, Phys. Chem. Chem. Phys. 5 (2003) 1717.
[8] D. Mathur, Phys. Rep. 225 (1993) 193.
[9] N. Lambert, D. Kearney, N. Kaltsoyannis, S.D. Price, J. Am. Chem. Soc. 126 (2004) 3658.
[10] D. Kearney, S.D. Price, Phys. Chem. Chem. Phys. 5 (2003) 1575.
[11] N. Lambert, N. Kaltsoyannis, S.D. Price, J. Žabka, Z. Herman, J. Phys. Chem. A 110 (2005) 2898.
[12] Z. Dolejšek, M. Fárník, Z. Herman, Chem. Phys. Lett. 235 (1995) 99.
[13] J. Roithova, D. Schröder, Phys. Chem. Chem. Phys. 9 (2007) 2341.
[14] J. Roithová, C.L. Ricketts, D. Schröder, S.D. Price, Angew. Chem. Int. Ed. 46 (2007) 9316.
[15] V. Vuitton, R.V. Yelle, P. Lavvas Philos, Trans. R. Soc. London, Ser. A 367 (2009) 729.
[16] J. Lilensten, C. Simon Wedlund, M. Barthélémy, R. Thissen, D. Ehrenreich, G. Gronoff, O. Witasse, Icarus 222 (2013) 169.
[17] R. Thissen, H. Soldi-Lose, C. Alcaraz, O. Dutuit, J. Zabka, J. Roithove, Z. Herman, P. Francesi, D. Bassi, Molecular Dication Reactions of Interest for Planetary Ionosphere, in Conference on Surface and Atomic Physics (SASP), La Thuile, Italy, 2004.
[18] J.F. Lockyear, C.L. Ricketts, M.A. Parkes, S.D. Price, Chem. Sci. 2 (2011) 150.
[19] C.L. Ricketts, S.M. Harper, S.W.-P. Hu, S.D. Price, J. Chem. Phys. 123 (2005) 134322.
[20] S.D. Price, Int. J. Mass Spectrom. 260 (2007) 1.
[21] M.A. Parkes, J.F. Lockyear, S.D. Price, D. Schroder, J. Roithova, Z. Herman, Phys. Chem. Chem. Phys. 12 (2010) 6233.
[22] M.A. Parkes, J.F. Lockyear, S.D. Price, Int. J. Mass Spectrom. 280 (2009) 85.
[23] J.F. Lockyear, M.A. Parkes, S.D. Price, J. Phys. B 42 (2009).
[24] W.P. Hu, S.M. Harper, S.D. Price, Mol. Phys. 103 (2005) 1809.
[25] W.-P. Hu, S.M. Harper, S.D. Price, Meas. Sci. Technol. 13 (2002) 1512.
[26] L. Wåhlin, Nucl. Instrum. Meth. 27 (1964) 55.
[27] J.H.D. Eland, Meas. Sci. Technol. 4 (1993) 1522.
[28] A. Oelsner, O. Schmidt, M. Schicketanz, M. Klais, G. Schönhense, V. Mergel, O. Jagutzki, H. Schmidt-Böcking, Rev. Sci. Inst. 72 (2001) 3968.
[29] M.A. Parkes, J.F. Lockyear, S.D. Price, Int. J. Mass Spectrom 354 (2013) 39.
[30] Z. Herman, Int. Rev. Phys. Chem. 15 (1996) 299.
[31] J.K. Bohlke, J.R. de Laeter, P. De Bievre, H. Hidaka, H.S. Peiser, K.J.R. Rosman, P.D.P. Taylor, J. Phys. Chem. Ref. Data 34 (2005) 57.
[32] J. Roithová, J. Žabka, J. Hrušák, R. Thissen, Z. Herman, J. Phys. Chem. A 107 (2003) 7347.
[33] S.M. Harper, S.W.P. Hu, S.D. Price, J. Chem. Phys. 120 (2004) 7245.
[34] S.J. King, S.D. Price, Int. J. Mass Spectrom 277 (2008) 84.
[35] S.M. Harper, S.W.P. Hu, S.D. Price, J. Chem. Phys. 121 (2004) 3507.
[36] C.L. Ricketts, The reactions of the molecular nitrogen doubly charged ion with neutral molecules of relevance to planetary ionospheres (PhD thesis), UCL, 2007.